Telecommunication System for Spacecraft Deorbiting Devices

Luca Simone Ronga, Simone Morosi(✉), Alessio Fanfani, and Enrico Del Re

University of Florence - CNIT, Via S. Marta 3, 50139 Florence, Italy
luca.ronga@cnit.it, simone.morosi@unifi.it

Abstract. In mission critical scenarios, fast and correct data reception is a crucial feature of telecommunication systems: particularly, to cope with unknown and fast variable channel state condition, with large Doppler shifts and low available power, incoherent and computationally light modulation techniques have to be considered. This paper deals with the design of suitable systems for a specific application fields, namely control operation of a satellite while it is placed into its orbit and the disposal of a satellite at the end of its life or the deep-space missions; moreover, a digital implementation of a receiver, based on DD-PSK modulation, is introduced which is perfectly compliant with these requirements.

Keywords: DD-PSK · Decommissioning · Deorbiting · Digital receiver

1 Introduction

In the next years, an easier space access by means of new low-cost satellite solutions such as micro or nanosatellites, could drive technology advances in communications. End-users and also satellite operators will take advantage of these opportunities. The grow of innovative satellite technologies will increase the global offer of broadcast telecommunication services [1].

The most interesting orbits for space based activities, namely GEO and LEO ones, are getting crowded by an huge number of space debris. Space debris are man-made objects like as dead satellites, upper stages, pieces from fragmentation or collision of parts and so on. Today the number of that space debris fragments is higher than some hundred million, as depicted in Table 1, and is growing exponentially [2]. Consequently, space debris may start colliding into each other and thus increasing the already high number of debris, towards a sort of collision reaction, known also as Kessler Syndrome that may lead to a space saturation [3].

Recent debris mitigation guidelines suggest to dispose and passivate a satellite at the end of its life [4,5]. This goal requires the use of a reliable communication link also when the satellite has limited functionalities, with a random and uncontrollable attitude or when the satellite could be defunct. In this scenario, the channel conditions may change rapidly, e.g., signal's amplitude could drop down or go up according to satellite tumbling rate. From a more general point of view, typical satellite channel impairments like heavy Doppler effect, phase

I. Bisio (Ed.): PSATS 2014, LNICST 148, pp. 45–57, 2016.
DOI: 10.1007/978-3-319-47081-8_5

Table 1. Estimated orbital population

Size	Number	Mass %
>10 cm	>30,000	99.93
1 − 10 cm	>750,000	0.035
<1 cm	>166,000,000	0.035
Total	>166,000,000	6,000 tonnes

distortion, harshly impair signal propagation: in these contexts traditional signal acquisition and synchronization techniques could end up being slow and inappropriate. In this paper a robust transmission technique is proposed which is based on the DD-PSK modulation [6]: this incoherent solution results to be extremely suitable for this context. Another positive feature of DD-PSK is the simple receiver's architecture: the absence of a PLL or of a carrier acquisition's circuits limits the system complexity.

This study is the result of a cooperation between University of Florence and D-Orbit S.r.l., an Italian company that develops a smart satellite device that decommissions satellites at the end of their operative life.

The paper is organized as follows: Sect. 2 provides an overview of the application's scenario and an estimation of the link budget. Section 3 proposes a complete description of the DD-PSK modem architecture and an analytical analysis of its operative principles. Section 4 discusses the performance of the whole transceiver architecture and shows the simulated results which have been obtained. Finally, conclusive remarks are given in Sect. 5.

2 Scenario

This section describes a possible scenario for a satellite decommissioning application. The goal is the design of a Telemetry and Tele-Command link (TM/TC) for a satellite placed in a polar Low Earth Orbit. The operative frequency is in S-Band: in particular ITU radio regulamentation and satellite standard [7,8] reserve the following sub-range:

- Frequency range: 2025 − 2110 MHz for Earth to space link;
- Frequency range: 2200 − 2290 MHz for space to Earth link.

The choose of S-band frequency was validated by a tradeoff analysis that has excluded the possible use of higher operative frequency, such as the X-Band (8 to 12 GHz). The major benefit of the use an X-band frequency is the considerably smaller physical dimension for the antenna that simplifies the integration on the satellite. On the other hand, the use of higher frequency brings stronger attenuations: the pathloss is increased by 14 dB and the link is greatly affected by other impairments such as ionospheric effects, scintillation, rain and fog attenuation [9]. Moreover, frequency value influences the performance of a ground station

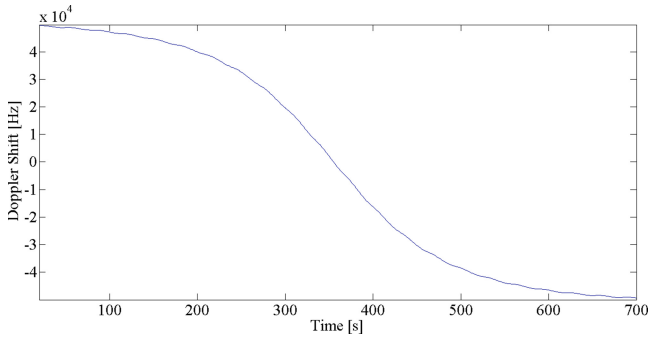

Fig. 1. Doppler shift S-curve

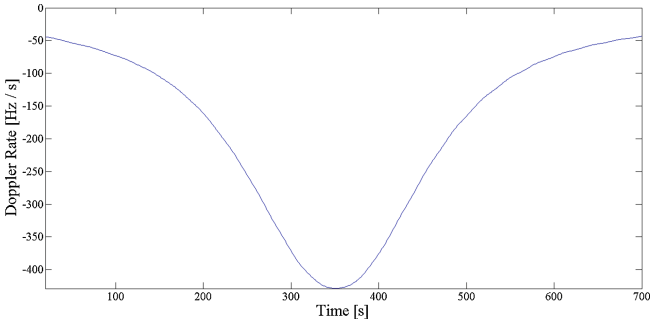

Fig. 2. Shift Doppler time variation

antenna: with an X-band frequency the HPBW angle becomes smaller and this consequently increases link's pointing losses; finally, the higher the frequency link, the higher the Doppler shift.

In LEO orbit the main channel impairment is due to the large and time-variant Doppler shift within a visibility window of satellite. The frequency shift can be represented by the S-curve, which is shown in Fig. 1: the maximum shift is within ±50 kHz. Another important figure is the Doppler shift rate that represents the time-variation of shift. The curve in Fig. 2 describes this feature: the worst case is achieved in the center of visibility window, when the satellite is closer to the ground station, and the Doppler rate is lower than −400 Hz per second.

The previous figures are compliant with CCSDS raccomandations, [8], that suggest a frequency acquisition range of at least ±150 kHz at 2 GHz and a minimum frequency sweep rate of 100 Hz/s.

The satellite is equipped with an hemispherical patch antenna dedicated to TM/TC link with antenna boresight allined with yaw satellite's axis. This configuration provides a stable signal only when satellite is in cruise mode, with a working attitude control system. With these hypothesis, the received power is

easily computed by means of standard link budget equation [9–11].

$$\frac{C}{N_0} = EIRP_{TX}\left(\frac{1}{L}\right)\left(\frac{G}{T}\right)_{RX}\left(\frac{1}{k}\right) \tag{1}$$

Equation 1 define the C/N_0 ratio that is directly related to E_b/N_0 by means of formula in Eq. 2.

As for the other parameters in previous equation, we can assume that:

- $EIRP_{TX}$ is the Equivalent Isotropically Radiated Power of the transmitter;
- L summarizes all the link attenuations;
- k is the Boltzmann constant;
- the receiving station's figure of merite G/T is function of antenna noise temperature T_A and noise figure of the receiver;
- $R_b = 1/T_b$ is the bit rate of the link (Table 2).

$$\frac{E_b}{N_0} = \frac{C}{N_0}\frac{1}{R_b} \tag{2}$$

Table 2. Link budget table

Parameters	Uplink	Downlink
	Worst Case	Worst Case
Satellite Slant Range [km]	2500	2500
Link Frequency [MHz]	2025	2200
Rate [kbps]	128	128
Transmitter Power [dB]	13.01	3.01
TX Antenna Gain [dB]	35	6
PathLoss [dB]	166.5	167.2
Polarization Loss [dB]	3	3
De-Pointing Loss [dB]	2.7	2.7
Atmospheric Loss [dB]	0.3	0.3
Scintillation Loss [dB]	10	10
RX Antenna Gain [dB]	6	35
Interconnection Loss [dB]	2.8	2.8
Noise Temperature [dBK]	27.8	13.7
EIRP [dB]	48.01	9.01
Figure of Merit [dB/K]	−21.8	21.3
Received Power [dBm]	−102.3	−112
C/N_0 [dB]	74.9	65.25
E_b/N_0 [dB]	23.9	14.18

In Fig. 3(a) and (b) the received power and the signal to noise ratio E_b/N_0 are represented in a visibility windows. These graphics are associated to a satellite with a perfectly working attitude control system. Such condiction is not always verified. For example, before the attitude stabilization or at the end of mission due to a fail of attitude control system, the satellite could casually lose stability. In this scenario, the channel results to be very unstable and the signal strength would follow the antenna radiation pattern dropping out completely when the antenna rotates away from ground station [12]. Figure 4(a) and (b) report the values of the previously considered curves as given by the link budget curves in a possible critical scenario. A high tumble rate has been supposed around all satellite's axes. The presumed angular rotation velocities are 20 deg/sec around Pitch axis, 10 deg/sec around Roll axis and 5 deg/sec around Yaw axis. A sequence of impulses highlights the signal instability and an adequate signal power is obtained only in short burst intervals whose duration is often less than 1 s. In this condition, a frequency acquisition becomes very hard due to quick amplitude fluctuations so that incoherent demodulation techniques could be the only feasible solution.

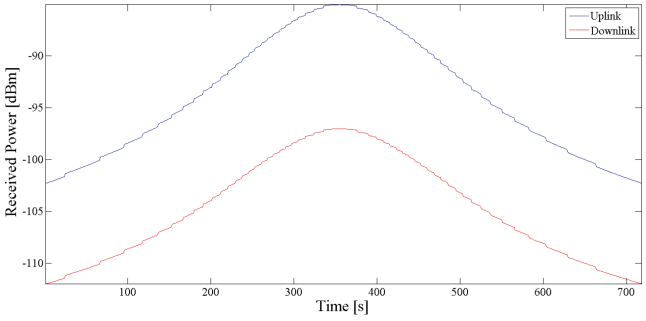

(a) Received Power

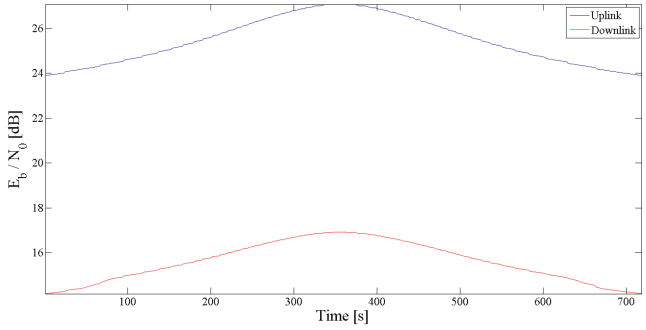

(b) Signal to Noise Ratio

Fig. 3. Link budget curve in stable attitude condition

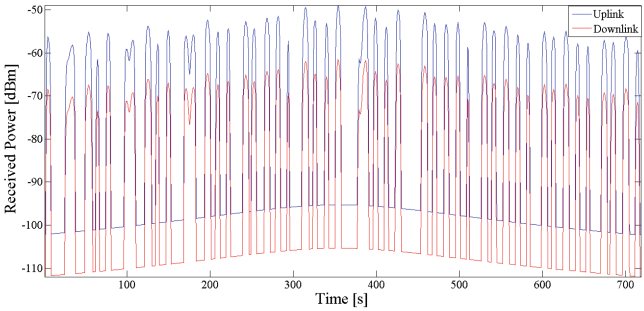

(a) Received Power

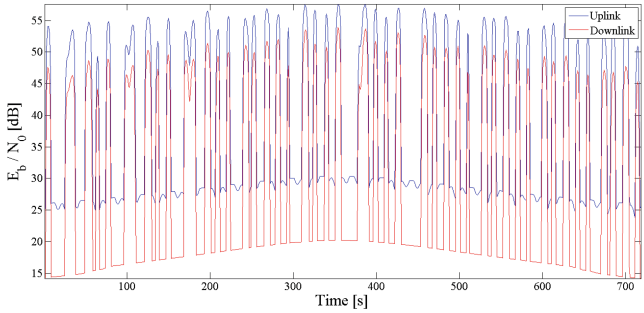

(b) Signal to Noise Ratio

Fig. 4. Link budget curve at the satellite's end of life

3 Communication Protocol

This section describes a possible communication protocol which is used to establish the link between the ground station and the decommissioning device installed on satellite. The transmission is a typical half-duplex communication, coming from the Ground Station that is the *Master Node*. The transceiver on satellite, *Slave Node*, is in receiving mode and it's ready to reply at each request from ground station. The approach is similar to a burst communication: Master and Slave node transmit short messages both in Up-Link and Down-Link.

Each message includes 223 bytes of useful information data. This message is then processed with a Reed Solomon (223,255) coding, a scrambling function and a convolutional coding with code rate equal to $\frac{1}{2}$. The final packet dimension becomes 530 byte. The whole channel coding chain is depicted in Fig. 5.

Supposing that a complete communication session include 10 messages exchange in both directions (Up-Link and Down-Link) and a session period is 1 s, as previously described, the minimum transmission rate is computed equal to 81600 bit per second. So, the desired transmission Rate has been defined equal to $2^{17} = 131072$ b/s.

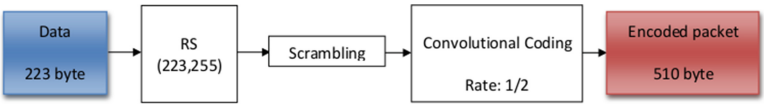

Fig. 5. Channel coding

4 Transceiver Architecture

The proposed transceiver architecture encompasses an analog front-end with a duplexer to divide receive and transmission chains, an IF section and a digital section implemented on a FPGA. A high level functional block of the transceiver is depicted in Fig. 6

The main functionalities which are implemented in the digital section are the signal modulation/demodulation, the IF to baseband frequency convertion and the frame coding/decoding.

The selected modulation is the Double Differential PSK (DD-PSK). Thanks to the double differential step, it's possible to demodulate the IF signal without a frequency acquisition or a phase estimation, even with a heavy Doppler shift [13]. This incoherent demodulator facilitates the implementation, increases the receiver's reliability and reduces the power consumption [6].

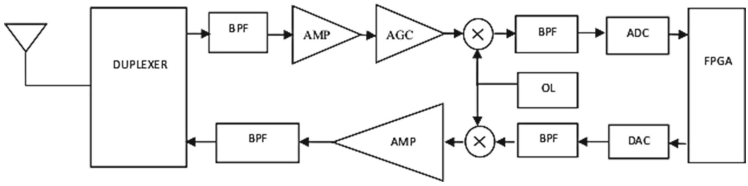

Fig. 6. Transceiver block diagram

4.1 Transmitter

The transmitted signal is PSK modulated; its information messages dictates the phase difference between three consecutive bits. The block representation of the DD-PSK modem is depicted in Fig. 7.

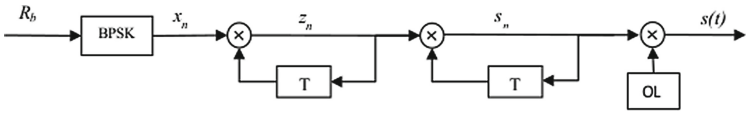

Fig. 7. DD-PSK modulator

The first B-PSK stage associates to bit "1" a phase value $\varphi_n = 0$ and to bit "0" a phase value $\varphi_n = \pi$. Thereafter, the double differential step creates the DD-PSK signal that is converted to a radio frequency value, f_{OL} into S-band. The delay blocks introduce a delay equal to the symbol period $T = 1/R_b$.

The analytical form of the signal is:

$$x_n = e^{i\varphi_n} \tag{3}$$

$$z_n = x_n x_{n-1} = e^{i\varphi_n} e^{i\varphi_{n-1}} = e^{i\Delta\varphi_n} \tag{4}$$

$$s_n = e^{i\Delta\varphi_n} e^{i\Delta\varphi_{n-1}} = e^{i\Delta^2\varphi_n} \tag{5}$$

$$s(t) = A\cos(2\pi f_{OL} t + \Delta^2\varphi_n) \tag{6}$$

where:

φ_n is the phase of bit n;

$\Delta\varphi_n = \varphi_n - \varphi_{n-1}$ is the first order difference;

$\Delta^2\varphi_n = \Delta\varphi_n - \Delta\varphi_{n-1} = \varphi_n + 2\varphi_{n-1} + \varphi_{n-2}$ is the second order difference.

4.2 Receiver

The receiver implementation works at Intermediate Frequency IF and uses a delayed reply of the same signal to down-convert it to base band.

An important design parameter is the sampling frequency. In order to avoid the overlapping of frequency images, the relationship between the sampling frequency and the IF frequency is described by the following equation:

$$f_c = \frac{4f_{IF}}{2n+1}, \; n = 0, 1, 2, .. \tag{7}$$

In Fig. 8 the spectrum of the sampled signal is depicted for $n = 0$: no signal overlapping is shown.

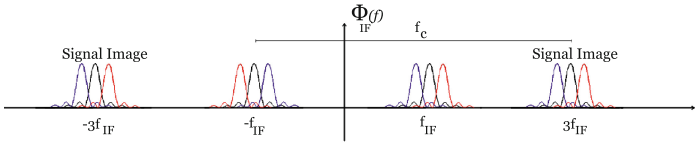

Fig. 8. Spectrum of the sampled signal

The value of transmission rate is assumed equal to an integer divisor of the sampling frequency: particularly, the relationship is defined by the equation $f_c = 128 \cdot R_b$; in every bit period there are 128 samples. In Table 3 all design parameters for the receiver are summarized.

The core of the receiver is the DD-PSK demodulator characterized by the two differational steps, which are depicted in Fig. 9. The main blocks of the demodulator are:

Table 3. Receiver design parameters

Transmission rate	$2^{17} = 131072\,\text{b/s}$
Intermediate frequency	$2^{22} = 4,194\,\text{MHz}$
Sample frequency	$2^{24} = 16,777\,\text{MHz}$
Maximum shift Doppler	150 KHz

– the delay blocks T_b;
– the *integrate and dump*, activated by the synchronization circuit;
– the threshold comparator for the bit detection.

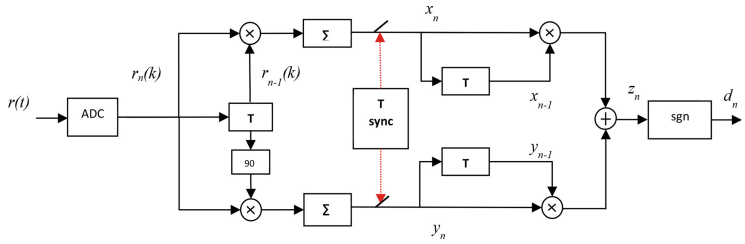

Fig. 9. Diagram of DD-PSK demodulator

The input signal, without noise contribute, is defined by the following equation:

$$r(t) = A\cos(2\pi((f_{IF} + \Delta f_{D_n})(t - \tau_{ch_n})) + \theta_n + \varphi_n) \tag{8}$$

where:

φ_n is the phase of bit n;
f_{IF} is the Intermediate Frequency;
Δf_{D_n} is the shift Doppler on bit n;
τ_{ch_n} is the channel delay on bit n;
θ_n is the phase error on bit n.
By means of several analytical computations, the final receiver output signal is:

$$d_n = sgn[\frac{T_b^2 A^4}{4}\cos\Delta^2\varphi_n] \tag{9}$$

Equation clearly shows that the result is independent from the Doppler Shift and/or the channel phase error: particularly, the output depends only on the two previous bits and their phase difference $\Delta^2\varphi_n$.

5 System Performance

A demonstration of DD-PSK robustness against the Doppler effect is obtained through a complete simulation of the receiver. The simulation has been performed in Simulink and the results are reported in Fig. 10. The bit error rate

curves are nearly constant for different Doppler conditions. The results have been obtained using a random binary transmitted sequence which is formed by 10^7 bits.

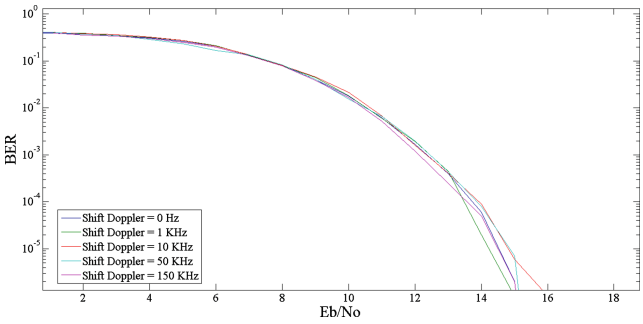

Fig. 10. DD-PSK demodulator performance

As demonstrated in paper [13], the performance of a DD-PSK demodulator can be computed as in Eq. 10.

$$P_{e_{DD-PSK}} = \exp[-\frac{E_b}{2N_0}(1 + \frac{N_0}{2E_b})^{-1}] \tag{10}$$

The DD-PSK Bit Error Probability is plotted in Fig. 11 where it is compared with BER curves of other binary modulations. Figure 11 shows that DD-PSK performance, in terms of Bit Error Rate, are about 4 dB lower than B-PSK coherent demodulation. This weakness could be exceeded introducing efficient channel coding techniques.

Finally, it's important to observe that the theoretical BER curves in Fig. 11 correspond with simulated results depicted in Fig. 10.

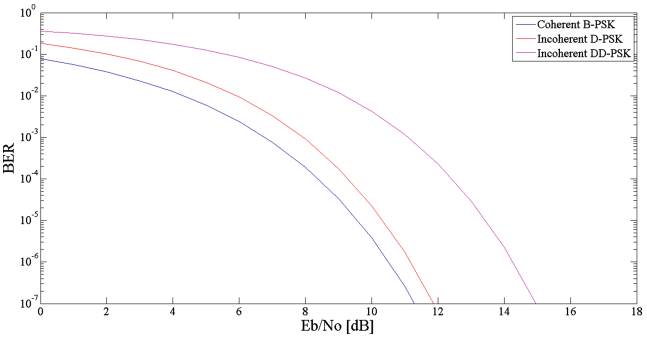

Fig. 11. Bit Error Rate for different modulation

5.1 Time Synchronization

In this section the synchronization issues are evaluated: they are deemed as a key element in the receiver design.

In the previous sections, the demodulator derivation is performed by assuming perfect synchronization. A key aspect of the DD-PSK receiver can be identified in the correct demodulation which can be performed with no signal preacquisition. Thanks to this peculiar feature this receiver can be proven robust in scenario with quick channel variations with no need to resort to long preamble sequences. An effective synchronization circuit will help to preserve this property and minimize acquisition time. The adopted frame of 512 bits is composed by a short preamble (16 bit), followed by the payload. When the preamble is acquired, the synchronization circuit generates a brief pulse that reset the *Integrated and Dump* in the demodulator. An example of this signal is represented in Fig. 12: the impulse period is nearly equal to 4.5 µs that is the frame period.

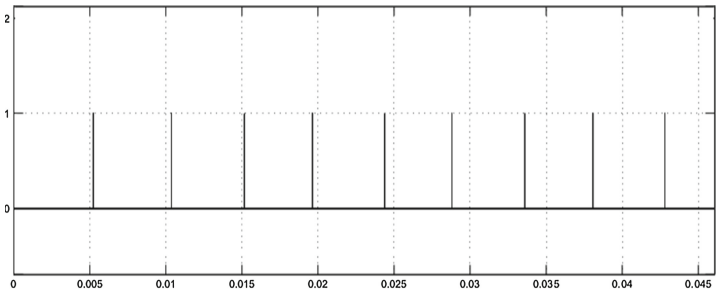

Fig. 12. Synchronization signal generated by Synchronization circuit

The performance of synchronization circuit is analyzed in Fig. 13. These curves show the frame loss probability, that is a missed preamble acquisition, in function of signal to noise E_b/N_0 and Doppler shift. We can conclude that the proposed synchronization circuit is insensitive to Doppler shift up to 50 kHz and it shows a satisfactory performance when E_b/N_0 is greater than 9 dB.

5.2 Overall Performance

The results of the whole receiver are shown in the following. To this aim we report the Bit Error Rate curves which are depicted in Fig. 14. The obtained BER results are similar to the curves in Fig. 10, i.e., the ones which are associated to an ideal DD-PSK demodulator. This result demonstrates the effectiveness of the global receiver architecture.

A further improvement of receiver performance is obtained by introducing channel signal coding [14]. An explanatory example of the improvement is given by BER curve in Fig. 15. In these simulation, the frame has been encoded with

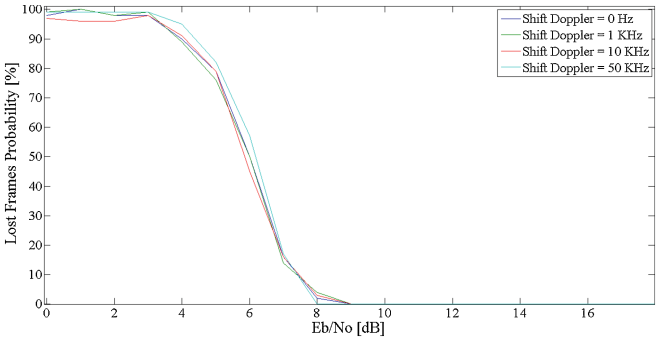

Fig. 13. Lost frame probability

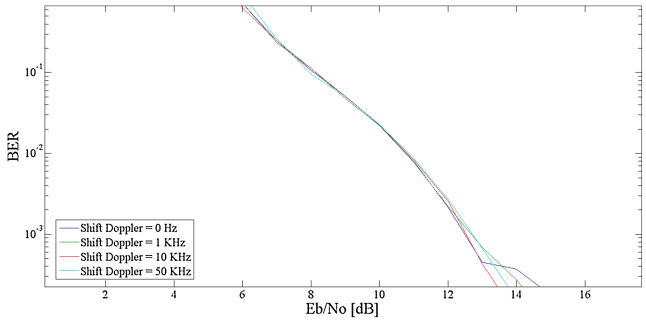

Fig. 14. Total receiver Bit Error Rate

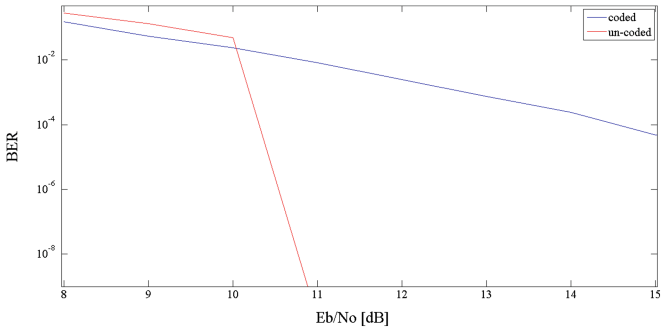

Fig. 15. Bit Error Rate with coded and uncoded frame

a Reed-Solomon (255,223) and a convolutional coding with coding rate equal to 1/2. The performance increase is significant: with a signal to noise ratio, E_b/N_0, greater than 10 dB, the final Bit Error Rate is less than 10^{-8}.

6 Conclusion

This paper analyzes the possible channel conditions in mission critical scenarios and proposes a modem architecture for a reliable earth-space telemetry communication link which is based on the DD-PSK modulation and is able to meet the system requirements. The proposed solution has been validated through computer simulations considering all the potential impairments in the chosen scenario or in a deorbiting mission: the incoherent feature and the robustness to Doppler of the DD-PSK simplify the receiver architecture and afford a reliable link also in emergency scenario.

References

1. Morosi, S., Jayousi, S., Del Re, E.: Cooperative delay diversity in hybrid satellite/terrestrial DVB-SH system. In: Proceedings of 2010 IEEE International Conference on Communications, ICC 2010, Cape Town, South Africa (2010)
2. Reflections on Orbital Debris Mitigation Measures Prof. Richard Crowther. Chief Engineer, UK Space Agency
3. Scientist: Space weapons pose debris threat CNN, 03 May 2002. Articles.cnn.com. Accessed 17 Mar 2011
4. IADC Space Debris Mitigation Guidelines, 25 October 2002
5. European Code of Conduct for Space Debris Mitigation, 28 June 2004. Issue 1.0
6. Yuce, M.R., Liu, W., Damiano, J., Bharath, B., Franzon, P.D., Dogan, N.S.: SOI CMOS implementation of a multirate PSK demodulator for space communications. IEEE Trans. Circ. Syst. I Regul. Pap. **54**(2), 420–431 (2007)
7. ECSS-E-ST-50-05C Rev. 2: Radio Frequency and Modulation, ESA-ESTEC, 4 October 2011
8. CCSDS 401.0-B: Radio Frequency and modulation system, January 2013
9. Ippolito, L.J.: Satellite Communications Systems Engineering: Atmospheric Effects, Satellite Link Design and System Performance. Wiley (2008)
10. Maral, G., Bousquet, M.: Satellite Communications Systems: Systems, Techniques and Technology. Pearson Education, India (2009)
11. Wertz, J.R., Larson, W.J.: Space Mission Analysis and Design. Microcosm Press (1999)
12. Bruzzi, J.R., Jensen, J.R., Fielhauer, K.B., Royster, D.W., Srinivasan, D.K.: Telemetry recovery and uplink commanding of a spacecraft prior to three-axis attitude stabilization. In: 2006 IEEE Aerospace Conference (2006)
13. Ma, C., Wang, D.: The performance of DDPSK over LEO mobile satellite channels. In: Proceedings of the 2000 Asia-Pacific Microwave Conference (2000)
14. Shu, L., Costello, D.J.: Error Control Coding. Pearson Education, India (2005)